

## The formation of pigeonite on the join hedenbergite–ferrosilite at 11.5 and 15 kbar: experiments and a solution model

DONALD H. LINDSLEY

*Department of Earth and Space Sciences  
State University of New York  
Stony Brook, New York 11794*

### Abstract

The three-pyroxene assemblage orthoferrosilite (OFs)-pigeonite (Pig)-hedenbergite ( $Hd_{ss}$ ) is stable on the  $CaFeSi_2O_6$ – $Fe_2Si_2O_6$  join at pressures above 11.5 kbar and below approximately 20 kbar. It is found at  $825 \pm 10^\circ C$  (11.5 kbar) and at  $855 \pm 10^\circ C$  (15 kbar). At lower pressures the low-Ca pyroxenes decompose to  $Hd_{ss}$  + Fayalite + Quartz while at and above 20 kbar the  $Hd_{ss}$  + Pig pair is replaced by a single clinopyroxene (Cpx). Under the assumption that (a) Pig has the  $C2/c$  space group at elevated temperatures and (b) Ca enters only the M2 site of Cpx, the Cpx solution can be described by an asymmetric Margules model:

$$G^{XS} = [(20.697 - 0.00235P)X_{CFs} + (16.941 + 0.00592P)X_{Hd}]X_{Hd}X_{CFs},$$

where units are kJ and kbar, and  $X_{CFs}$  and  $X_{Hd}$  are the mole fractions of  $Fe_2Si_2O_6$  and of  $CaFeSi_2O_6$  in Cpx. The Gibbs free energy for the reaction  $OFs = CFs$  ( $C2/c$ ) is given by

$$\Delta G_1 = +1.843 - 0.001676T(\text{Kelvin}) + 0.03686P \text{ kJ.}$$

The Opx solution is assumed to be symmetric, with  $W_G = 15$  kJ.

### Introduction

The join  $CaFeSi_2O_6$ – $Fe_2Si_2O_6$  (Hd–Fs) has been of interest to petrologists mainly because it is the Mg-free boundary of the pyroxene quadrilateral. Based on pyroxene assemblages found in a variety of igneous and metamorphic rocks, one might expect the Hd–Fs join to show several two-pyroxene fields—orthopyroxene + high-Ca clinopyroxene (OFs +  $Hd_{ss}$ ), OFs + low-Ca Cpx (Pig), and  $Hd_{ss}$  + Pig—as well as the three-pyroxene assemblage  $Hd_{ss}$  + Pig + OFs. Experimental calibration of the phase compositions and temperatures for these assemblages would greatly aid in interpreting natural pyroxenes, either by graphical extrapolation or by use of a thermodynamic solution model for Ca–Fe pyroxenes as a boundary for a model of more complex pyroxenes.

However, it has been known since the pioneering study of Bowen, Schairer, and Posnjak (1933) that pyroxenes are stable on this join at 1 atm only for compositions close to  $CaFeSi_2O_6$ . Lindsley and Munoz (1969) found that increasing pressure stabilizes increasingly iron-rich pyroxenes, and they

showed pyroxenes as stable (relative to olivine (Fa) and quartz (Q)) over the entire join at 20 kbar. The recent careful study of Bohlen, Essene, and Boettcher (1980) showed that pure  $Fe_2Si_2O_6$  is not stable below *ca.* 12–13 kbar in the temperature range considered here (800–1000°C). The presence of Ca stabilizes OFs to slightly lower pressures, but direct experimental determinations of two- and three-pyroxene equilibria on the Hd–Fs join are limited to pressures at or above 11.5 kbar.

A number of workers (*e.g.*, Bowen *et al.*, 1933; Turnock, 1962; Lindsley, MacGregor, and Davis, 1964; Lindsley, 1967; Lindsley and Burnham, 1970) have found that, with increasing temperature, pyroxenes on the Hd–Fs join may transform to pyroxenoids. This paper is not concerned with pyroxenoids; it deals with temperatures sufficiently low (800–1000°C) to keep pyroxenes as the stable metasilicates.

The subsolidus phase diagram for the Hd–Fs join at 20 kbar is quite simple (Lindsley and Munoz, 1969, p. 308): below 800°C there is a broad field of hedenbergite solid solution ( $Hd_{ss}$ ) + OFs. From

approximately 850 to 950°C the Hd<sub>ss</sub> field widens rapidly, so that at 950°C the Hd<sub>ss</sub> (or Cpx) field extends from Hd to approximately Hd<sub>10</sub>Fs<sub>90</sub> (mole percent). Lindsley and Munoz searched for a stable two-Cpx (Hd<sub>ss</sub> + Pig) field but found none. Accordingly, they concluded that the Hd<sub>ss</sub>(OFs) solvus (that is, the curve showing the composition of Hd<sub>ss</sub> in equilibrium with OFs) is inflected, and their diagram is topologically similar to the subsolidus portion of that proposed by Davis and Boyd (1966) for the Diopside–Enstatite join at 30 kbar. Like Davis and Boyd, Lindsley and Munoz concluded that the inflected solvus resulted from the interference of a two-Cpx miscibility gap with the Opx–Cpx transition loop. This paper reports experiments at 11.5 to 15 kbar that demonstrate the existence of this miscibility gap at the lower pressures and that show the temperatures and compositions for the isobarically invariant three-pyroxene assemblages Hd<sub>ss</sub> + Pig + OFs on the Hd–Fs join. These data are combined with the earlier results at 20 kbar to yield a solution model for Ca–Fe pyroxenes.

### Experimental techniques

#### Starting materials

Pyroxenes for use as starting materials were synthesized by the methods of Turnock, Lindsley, and Grover (1973) using high-purity chemicals. Final synthesis conditions for each pyroxene are given in Table 1; most were made hydrothermally at 20–22 kbar and 950–980°C, in silver capsules, using a piston-cylinder apparatus with a 0.75" (1.91 cm) bore. Each capsule was 0.50" (1.27 cm) long and 0.25" (0.64 cm) in diameter, and was loaded with

approximately 0.4 g of prereacted pyroxene mix, 30 mg H<sub>2</sub>O, 2–3 mg SiO<sub>2</sub> glass, and 1–2 mg oxalic acid. The excess silica prevents desilication of the pyroxene by the hydrothermal fluid, and the oxalic acid breaks down to produce small amounts of reducing gases (CO, H<sub>2</sub>) that prevent oxidation of the pyroxene. Dry syntheses (Table 1) used Fe<sup>0</sup> capsules of the same size as the silver ones. Most were performed in the piston-cylinder apparatus, although the most calcic was made by crystallizing glass, the Fe capsule being held in an evacuated SiO<sub>2</sub>-glass tube.

The synthesized pyroxenes were checked for homogeneity and complete reaction by powder X-ray diffraction and by electron probe microanalysis. Table 1 shows the starting materials—single phases and mechanical mixtures of two pyroxenes—that were used to bracket the compositions of the coexisting phases and to determine the temperatures of the Hd<sub>ss</sub> + Pig + OFs assemblage.

#### Experiments

Approximately 10 mg of desired starting material, 1 mg of H<sub>2</sub>O, and 0.1 to 0.2 mg each of SiO<sub>2</sub> glass and of oxalic acid were loaded into silver capsules 0.094" (0.24 cm) in diameter by 0.140" (0.36 cm) long. A tightly fitting Ag lid was rammed into the capsule, and the upper lip of the capsule peened over the lid to provide a seal. The experiments were performed in a 0.5" (1.27 cm) piston-cylinder apparatus using a furnace assembly like that of Boyd and England (1963) but with four important differences: (1) No boron nitride sleeve was used; instead, the graphite furnace fit directly into the talc sleeve. This arrangement was made feasible both by the relatively low temperatures of the experiments and by their hydrothermal nature: any water released by dehydrating talc would not affect the charges; (2) the solid insert was AlSiMag222 (American Lava Co.) rather than boron nitride; (3) two capsules were placed end-to-end within the furnace assembly; and (4) the interface between the capsules, rather than the thermocouple junction, was placed at the center of the thermal profile of the furnace. Calibration experiments using multiple thermocouples and dummy capsules show that the hotter ends of each capsule were 12–15°C above the nominal temperature indicated by the Pt vs. Pt<sub>90</sub>Rh<sub>10</sub> thermocouple; the reported temperatures have been corrected for this difference.

The samples were taken at room temperature to nominal pressures 1.5 to 2.5 kbar above the desired

Table 1. Starting materials

Ref.	Composition	Phase(s)	Synthesis Conditions (or other source)		
			P (kbar)	T (°C)	Duration (h)
A	Fs <sub>100</sub>	Opx	22	930–960	8
B	Fs <sub>93</sub> Wo <sub>7</sub>	Cpx*	22	950–980	3
C	Fs <sub>90</sub> Wo <sub>10</sub>	Cpx*	20	950–980	2.5
D	Fs <sub>87</sub> Wo <sub>13</sub>	Opx+Cpx		(Mechan. Mix of A and L)	
E	Fs <sub>85</sub> Wo <sub>15</sub>	Cpx*	20	950–980	2.1
F	Fs <sub>80</sub> Wo <sub>20</sub>	Cpx	20	950–980	2
G	Fs <sub>77.5</sub> Wo <sub>22.5</sub>	2Cpx*		(Mechan. Mix of C and K)	
H	Fs <sub>75</sub> Wo <sub>25</sub>	Cpx**	20	1150–1190	1.5
I	Fs <sub>75</sub> Wo <sub>25</sub>	2Cpx		(Mechan. Mix of C and L)	
J	Fs <sub>75</sub> Wo <sub>25</sub>	Opx+Cpx		(Mechan. Mix of A and L)	
K	Fs <sub>65</sub> Wo <sub>35</sub>	Cpx**	15	1110–1150	2.3
L	Fs <sub>60</sub> Wo <sub>40</sub>	Cpx**	(evac)	900°	116

\*Trace of Opx seeds added.

\*\*Fe<sup>0</sup> capsule. Remaining syntheses were hydrothermal, in Ag capsules.

pressure, and then were taken to the desired temperature. During the initial stages of heating, the gauge pressure dropped but in the final stages it rose again. When the run temperature was reached, the gauge pressure was lowered to the appropriate value; thus, the experiments are of the outstroke type. Pressures were calibrated by bracketing the OFs = Fa + Q reaction at 825°C and comparing the results with those of Bohlen *et al.* (1980), who used NaCl pressure cells. These calibrations indicate that the apparent pressures in the present experiments were approximately 2 kbar too high for run durations similar to those by Bohlen *et al.* (24 hrs). The discrepancy slowly diminishes with increasing run duration (probably because of a slow relaxation of the talc pressure medium), and a correction of -1.5 kbar has been adopted.

#### Analysis

After quenching, the silver capsules were cleaned, weighed, and gently cut with a pair of end-nippers until a hiss—escaping gases from the oxalic acid—was heard. The capsule was then placed in a glass shell vial on a hot plate at approximately 120°C. Droplets of water condensing on the upper parts of the vial confirmed that the capsule had retained water, and a re-weighing usually showed that 85–90% of the original water was lost on the hot plate. Some of the balance remained in the sample as fluid inclusions. Further evidence that a fluid phase was present at *P* and *T* is the friable nature of the charges: the grains were not tightly sintered together in the fashion typical of dry high-pressure experiments.

The charges were examined in oil mounts under the petrographic microscope and by powder X-ray diffraction. If reaction appeared to have taken place, a portion of the charge was mounted in epoxy for electron probe analysis. Typical grain sizes were 5–30 microns for Cpx and 10–500 microns for Opx. (The largest Opx grains formed in runs where the starting material was low-Ca Cpx to which minute amounts of Opx seeds had been added. In common with many other investigators, I found Opx reluctant to nucleate, and seeding was essential to achieve equilibrium.)

The microprobe analyses were made on an automated ARL-EMX SM probe with on-line data reduction using the Bence-Albee and Albee-Ray correction procedures, an accelerating potential of 15kV, and a specimen current (on brass) of 0.015  $\mu$ A. Y-6 diopside and a synthetic Opx ( $Wo_4En_{24}Fs_{72}$ ) served

as standards. The fine grain size of some Cpx made analysis difficult, even using the minimum spot size ( $\approx 1$  micron). Analyses were accepted if the oxide sums were  $100 \pm 2$  wt.% and the cations summed to  $4.00 \pm 0.02$  per six oxygens; most analyses fell well within these limits. I also encountered problems with zoning and grain-overlap in some runs (*cf.*, Lindsley and Dixon, 1976). In particular, the analyses of Hd<sub>ss</sub> in some mechanical mixtures run at low temperatures differ little from the starting material, even though the X-ray diffraction patterns may show a considerable decrease in Ca content. This apparent discrepancy is clearly due to the tendency of the microprobe operator to direct the electron beam to the center of a small grain, thus maximizing the probability of analyzing a core of relic starting material. The X-ray powder pattern, in contrast, is dominated by the volumetrically more important rim of product pyroxene.

#### Results

The results of the experiments at  $11.5 \pm 0.5$  and at  $15 \pm 0.5$  kbar are shown in Table 2 and in Figure 1. In contrast to the results of Lindsley and Munoz (1969) at 20 kbar, there is a small but definite field of Hd<sub>ss</sub> + Pig at the lower pressures. (The reasons for the difference are discussed in a later section.) The isobarically invariant assemblage of Hd<sub>ss</sub> + Pig + Opx is constrained to be at  $825 \pm 10^\circ\text{C}$  (11.5 kbar) and  $855 \pm 10^\circ\text{C}$  (15 kbar). Analyses of Opx and of Pig tend to be tightly clustered, in part because larger grain size facilitated the analysis. Microprobe analyses of Hd<sub>ss</sub> formed at lower temperatures must generally be augmented by X-ray determinations of composition, so the Hd<sub>ss</sub> (Opx) solvus is not so tightly constrained as one would wish.

#### Solution model

The coexistence of three solutions in a binary join puts very tight constraints on thermodynamic solution models. The model for Hd-Fs presented here is very similar in form to that developed for the Di-En join by Lindsley, Grover, and Davidson (1981). It assumes (1) that pigeonite has the *C2/c* space group at elevated temperatures and thus Hd<sub>ss</sub> and Pig have the same equation of state; (2) that the Cpx solution is asymmetric; (3) that Ca is effectively excluded from the M1 site of Cpx and thus Hd serves as a true end member for the solution; Ca-Fe mixing takes place on the M2 site only; (4) that Opx behaves as a regular, symmetric solution. Assumption (1) is strongly supported by the high-tempera-

Table 2. Results of experiments

Ref. #	Start. Mtl.	P (Kbar)	T (°C)	Duration d. h.	R U N P R O D U C T S		
					X-ray	Microprobe (mole % Ca <sub>2</sub> Si <sub>2</sub> O <sub>6</sub> )	
					OFS	Pig	Hd
1	F	11.5	865	9 17	Pig+Hd	15-18	23-25
2	B	11.5	865	9 17	OFS+Pig	4-5.5	9-11
3	D	11	840	11 22	OFS+Pig	4.5-5.5	12-13
4	C	12	825	1 0	OFS+Pig	5	11-12
5	C	11.5	825	14 3	OFS+Hd	4.5-5.5	32-35
6	D	11	825	10 0	OFS+Hd	4-5	32-34
7	I	15	900	7 14	One Cpx (broad peaks)		{ 21-26 }
8	G	15	885	13 21	One Cpx? (broad peaks)		{ 19-27 }
9	B	15	885	13 21	OFS+Pig	4.5-5	12-13
10	D	15	865	8 21	Pig+OFS	4.5-5.5	13-15
11	B	15	865	8 21	OFS+Pig	4.5-5.5	15-16
12	D	15	855	14 0	OFS+Hd; (hint of Pig)	4-5	30-31
13	E	15	855	14 0	OFS+Hd (+Pig)	4.5-5	29-31
14	H	15	850	6 21	Hd+Opx (+Pig)	5.5	13-14 28.5-30
15	E	15	840	10 0	OFS+Hd [Wo <sub>30-35</sub> ]	4.5-6	---
16	D	15	840	10 0	OFS+Hd [Wo <sub>32-36</sub> ]	4-5	38-40
17	J	15	825	21 2	OFS+Hd [Wo <sub>35-37</sub> ]	4-5	33-40
18	F	15	825	21 2	OFS+Hd [Wo <sub>29-31</sub> ]	4-5	---
19	F	15	810	14 14	OFS+Hd	4.5-5.5	31.5-32.5
20	J	15	810	13 20	OFS+Hd	3-5	33-33.5

(Pig) means minor pigeonite interpreted as metastable exsolution from Cpx.

{21-26} compositional range of essentially homogenized Cpx.

[Wo<sub>30-35</sub>] composition of Hd from X-ray diffraction; given only where microprobe results are lacking or inconsistent.

All experiments in Ag capsules; hydrothermal conditions.

ture crystallography studies of Ohashi, Burnham, and Finger (1975) and (2) is required by the compositions of coexisting Hd<sub>ss</sub> and Pig. (3) is compatible with available experimental and crystallographic data, although the possibility of a small amount of Ca in Ml of Hd probably cannot be excluded. Assumption (4) is not critical; in common with recent modellers of the Di-En join (*e.g.*, Saxena and Nehru, 1975; Holland, Navrotsky, and Newton, 1979; Lindsley *et al.*, 1981), I found that the overall model was very little dependent on the expression adopted for Opx. This is mainly because the Opx free energy curve needs be fit over a very narrow range of composition close to Fe<sub>2</sub>Si<sub>2</sub>O<sub>6</sub>. I have arbitrarily adopted a value for  $W_G(\text{Opx})$  of 15 kJ.

The formalism of the solution model is presented extensively in Lindsley *et al.* (1981), and need not be repeated in detail here. The goal, of course, is to evaluate expressions for the Gibbs free-energy curves for two solutions—Cpx and Opx. Two-Cpx equilibria depend only on the shape of the Cpx  $G$ -curve. In contrast Cpx-Opx equilibria depend not only on the *shapes* of the curves, but upon the

relative stabilities of the end members. The relative positions of the ends of the curves are determined by the reactions



and



through the relations

$$\begin{aligned} \mu_{\text{Fs}}^{\text{O,Cpx}} - \mu_{\text{Fs}}^{\text{O,Opx}} &= \Delta G_1 = \Delta U_1 - T\Delta S_1 \\ &+ (P - 0.001)\Delta V_1 \end{aligned} \quad (3)$$

and

$$\begin{aligned} \mu_{\text{Hd}}^{\text{O,Cpx}} - \mu_{\text{Hd}}^{\text{O,Opx}} &= \Delta G_2 = \Delta U_2 - T\Delta S_2 \\ &+ (P - 0.001)\Delta V_2 \end{aligned} \quad (4)$$

where the units are kJ, Kelvin, kJ/Kelvin, kbar, and kJ/kbar. (Writing reaction 2 does not imply the stable existence of "orthohedenbergite", because  $\Delta G_2$  is always negative.  $W_G(\text{Opx})$  and  $\Delta U_2$  are highly (negatively) correlated, and the value of 15 kJ adopted for  $W_G(\text{Opx})$  ensures that the model will not predict the stability of "orthohedenbergite".)

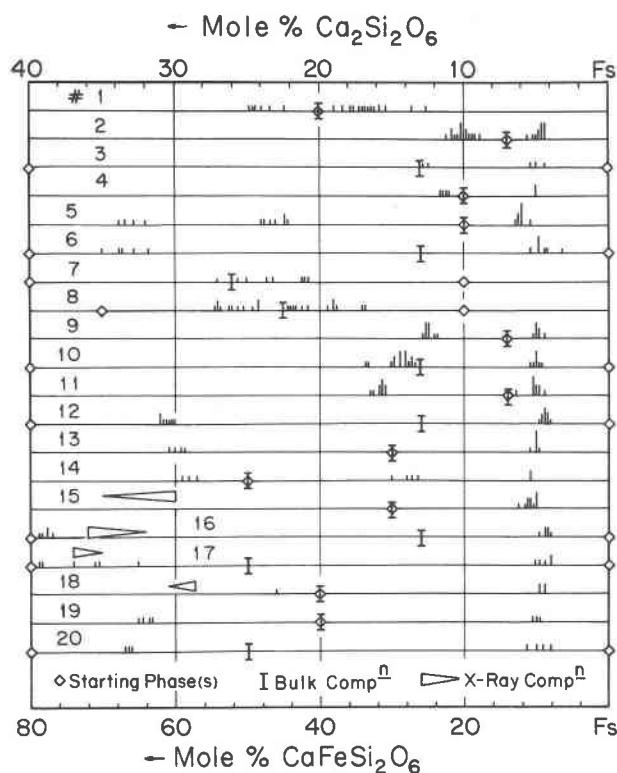


Fig. 1. Summary of microprobe analyses of run products for 11.5 and 15 kbar. Each "tick" represents one analysis. In a few runs (low temperatures at 15 kbar) the product  $Hd_{ss}$  was too fine-grained to probe, or analyses showed zoned starting material; for these cases compositions of  $Hd_{ss}$  are estimated from the (221), (310), (31 $\bar{1}$ ) and (311) powder X-ray diffraction peaks (triangular symbols).

For each two-pyroxene pair the equilibrium expressions are:

$$\mu_{Fe_2Si_2O_6}^A = \mu_{Fe_2Si_2O_6}^B \quad (5)$$

and

$$\mu_{CaFeSi_2O_6}^A = \mu_{CaFeSi_2O_6}^B \quad (6)$$

where the A-B pairs are  $Hd_{ss}$ -Opx, Pig-Opx, or  $Hd_{ss}$ Pig as appropriate. The three-pyroxene assemblages at 11.5 and 15 kbar require that:

$$\mu_{Fe_2Si_2O_6}^{Hd} = \mu_{Fe_2Si_2O_6}^{Pig} = \mu_{Fe_2Si_2O_6}^{Opx} \quad (7)$$

and

$$\mu_{CaFeSi_2O_6}^{Hd} = \mu_{CaFeSi_2O_6}^{Pig} = \mu_{CaFeSi_2O_6}^{Opx} \quad (8)$$

The appropriate expressions for the chemical potentials can be derived from equations on pp. 166-167 of Lindsley *et al.* (1981) by substituting Hd for Di and Fs for En<sup>1</sup>. The asymmetric Margules

<sup>1</sup> Please note, however, that  $W_{G1}$  and  $W_{G2}$  were inadvertently reversed in those equations.

parameters for the Cpx solution have the form:

$$W_{G_{12}} = W_{U_{12}} + PW_{V_{12}} \quad (9)$$

and

$$W_{G_{21}} = W_{U_{21}} + PW_{V_{21}} \quad (10)$$

(No excess-entropy term was required to fit the data). The right-hand sides of Eqs. 3-4 and 9-10 contain 10 unknowns. The relations among chemical potentials (Eqs. 5-8) provide a total of 42 equations in these unknowns for the experimental data at 11.5, 15, and 20 kbar. I solved these by a linear least-squares technique. The compositions used in the initial stages of the modelling were the mid-points of the experimental brackets. However, as argued by Lindsley *et al.* (1981), the mid-points are not necessarily the most appropriate compositions (*any* composition within a poorly determined bracket is acceptable), and the first sets of parameter values obtained were not compatible with the three-pyroxene equilibria (Eqs. 7, 8). Accordingly, I adjusted the compositions (within the limits of brackets) and repeated the least-squares procedure, until the parameters converged on values (Table 3) that were compatible with all the experiments, including the three-pyroxene equilibria. A test of the model was to calculate phase diagrams and to compare the calculated diagrams with the experimental data (Fig. 2).

An additional test of the model is to compare the predicted univariant curve for reaction 1 [OFs-CFs equilibrium] with experimental data. Because the model assumes that all compositions of Cpx have the  $C2/c$  space group, the Opx-low-Cpx ( $P2_1/c$ )

Table 3. Values of parameters for Hd-Fs solution model

Parameter	Value/mole	Error	Di-En*
$\Delta U_1$ (kJ)	1.843	0.061	3.561
$\Delta S_1$ (kJ/K)	0.00168	0.00006	0.00191
$\Delta V_1$ (kJ/kbar)	0.0369	0.0008	0.0355
$\Delta U_2$ (kJ)	-5.261	0.062	-21.178
$\Delta S_2$ (kJ/K)	0.00053	0.00005	-0.00816
$\Delta V_2$ (kJ/kbar)	-0.0951	0.0009	-0.0908
$W_U$ (CFs) (kJ)	16.941	0.062	25.484
$W_V$ (CFs) (kJ/kbar)	0.0059	0.0036	0.0812
$W_U$ (Hd) (kJ)	20.697	0.018	31.216
$W_V$ (Hd) (kJ/kbar)	-0.00235	0.0009	-0.0061
$W_G$ (Opx) (kJ)	15**		25**

Subscripts 1 and 2 refer to reactions (1) and (2).  
 $W_G(i) = W_U(i) + W_V(i) \cdot P(\text{kbar})$ , where (i) is Hd or CFs.

$CX^S(\text{Cpx}) = [W_G(\text{CFs})X_{Hd} + W_G(\text{Hd})X_{CFs}]X_{Hd}X_{CFs}$ .

(Notation follows convention of Thompson, 1967.)

\* From Lindsley *et al.* (1981) for comparison. Here reaction (1) refers to  $OE_n = CE_n$ , and CFs and Hd are replaced by  $CE_n$  and Di, respectively.

\*\* Assumed.

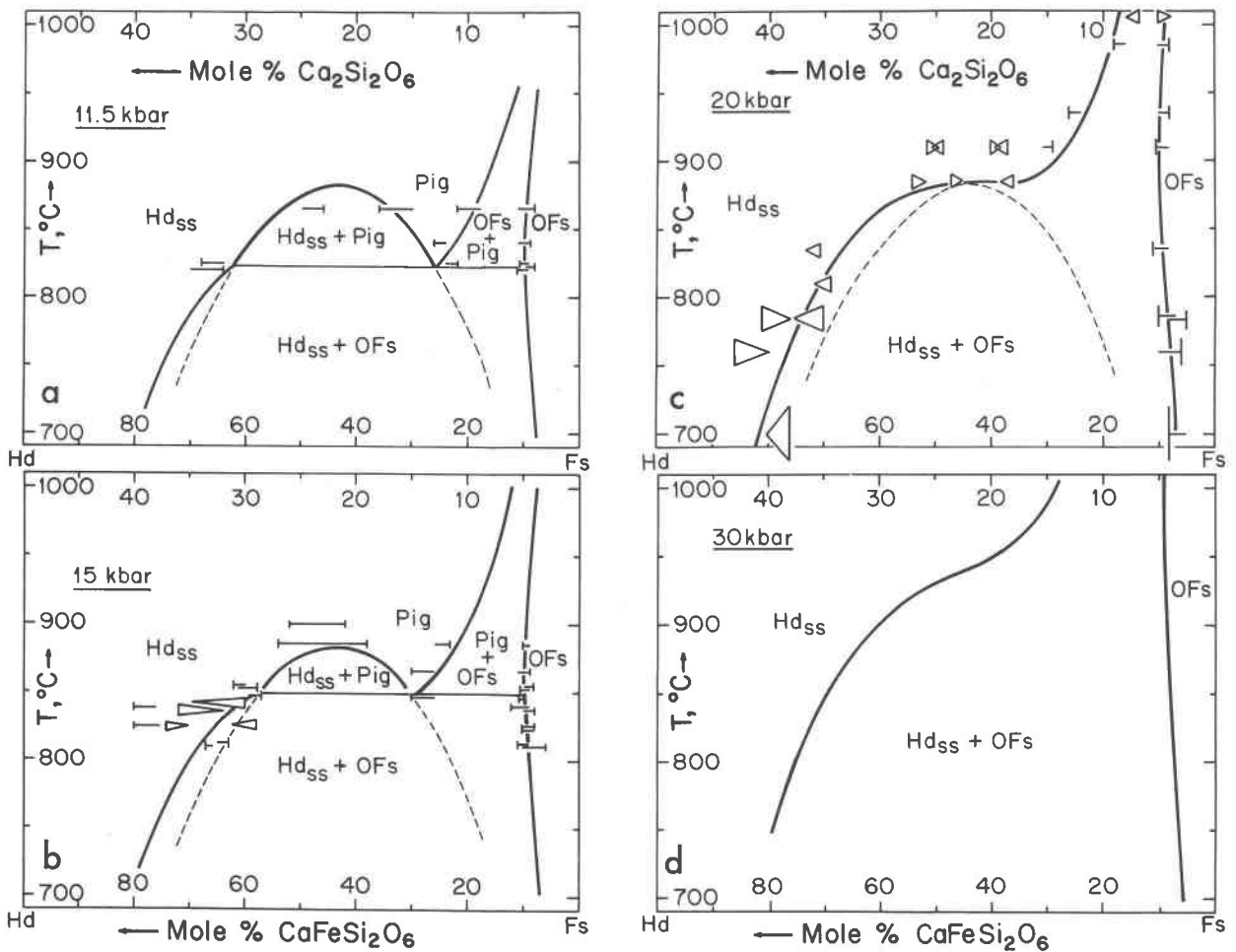


Fig. 2. Subsolidus phase diagrams for the Hd-Fs join calculated from the solution model and compared with the experimental data: 11.5 and 15 kbar, this paper; 20 kbar, Lindsley and Munoz (1969). Symbols:  $\dashv$  and  $\vdash$ , horizontal line shows range of composition for run products by microprobe analysis (Fig. 1; Table 2); vertical line shows direction from which equilibrium was approached. Arrowheads, compositions from X-ray determinative curves. a. 11.5 kbar. b. 1 kbar. c. 20 kbar. d. 30 kbar.

phase boundary is not germane, and, hence, the thermochemical parameters derived by Helgeson, Delaney, Nesbitt, and Bird (1978) for the latter reaction are not comparable with the present results. I have recently re-interpreted some old data on ferrosilite as indicating an Opx to high-Cpx (C2/c) reaction with increasing temperature in the range 28 to 42 kbar (Lindsley, 1980). That revised phase diagram and the Opx-Cpx boundary calculated from the solution model are presented in Figure 3. The agreement, while not perfect, seems satisfactory.

### Discussion

The solution model presented here is compatible with the available experimental data (11.5–20 kbar).

The change of topology of the phase diagrams—from the 3-pyroxene assemblage at 11.5 and 15 kbar (Figs. 2a,b) to the inflected Hd<sub>ss</sub> (Opx) at 20 kbar (Fig. 2c)—can be explained by the destabilization of Pig with increasing pressure. By approximately 20 kbar and 885°C, the consolute point on the Cpx G-curve has a tangent to the Opx G-curve and, hence, the two-Cpx field has disappeared. Lindsley *et al.* (1981) calculated an identical sequence of phase diagrams for the Di-En join, although there the two-Cpx field persists up to 21 kbar (Figs. 3a-f).

The CFs-Hd solution is asymmetric in the same sense as CEn-Di. However, the excess parameters for the Ca-Fe Cpx are smaller by 8–10 kJ than those for Ca-Mg Cpx, in keeping with petrologic observations that the two-Cpx field tends to narrow with

increasing Fe/Mg. (This tendency is only partly offset by the fact that temperatures in igneous rocks generally decrease with increasing Fe/Mg.).  $\Delta U$  for the OFs-CFs inversion is one-half that reported for OEn-CEn by Lindsley *et al.* (1981);  $\Delta V$  and  $\Delta S$  are closely comparable for both reactions.

Unit-cell volumes of Cfs-Hd pyroxenes measured at room temperature (for example, Lindsley, Munoz, and Finger, 1969) show a positive excess volume of mixing; the volume curve is everywhere concave downward. In contrast, the volume curve implied by the  $W_V$  parameters for Cpx in Table 2 is very slightly S-shaped with a small negative excess volume near  $\text{Fe}_2\text{Si}_2\text{O}_6$  (Fig. 4). Although the latter curve is only inferred rather than directly measured, it may be more appropriate for the solution model than is the measured curve, because the volumes are more likely to change upon quenching than are compositions of the solid phases. The signs of the  $W_V$  terms are the same as those found by Lindsley *et al.* (1981) for CEn-Di, but the excess volumes for Ca-Fe Cpx are distinctly smaller.

To the extent that one may extrapolate the volume data (both the  $V^{XS}$  and the  $\Delta V$  terms for reactions 1 and 2), the model presented here can be used to calculate metastable pyroxene relations on the Hd-Fs join at low pressures. As phase-equilibrium data on Ca-bearing olivines become available

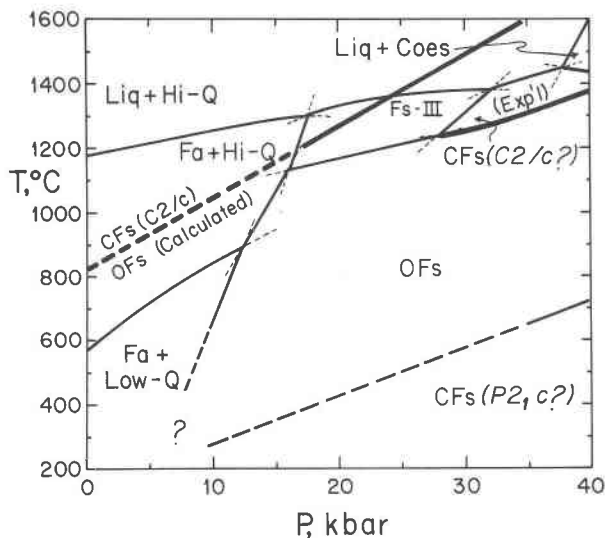


Fig. 3. Comparison of the phase-equilibrium diagram for  $\text{Fe}_2\text{Si}_2\text{O}_6$  (Lindsley, 1980, Fig. 2) and the OFs-CFs ( $C2/c$ ) inversion calculated from the parameters of reaction (1). The CFs is presumed to be  $C2/c$  at elevated temperatures. The calculated curve is in qualitative agreement with the experimentally determined one (heavy curved line).

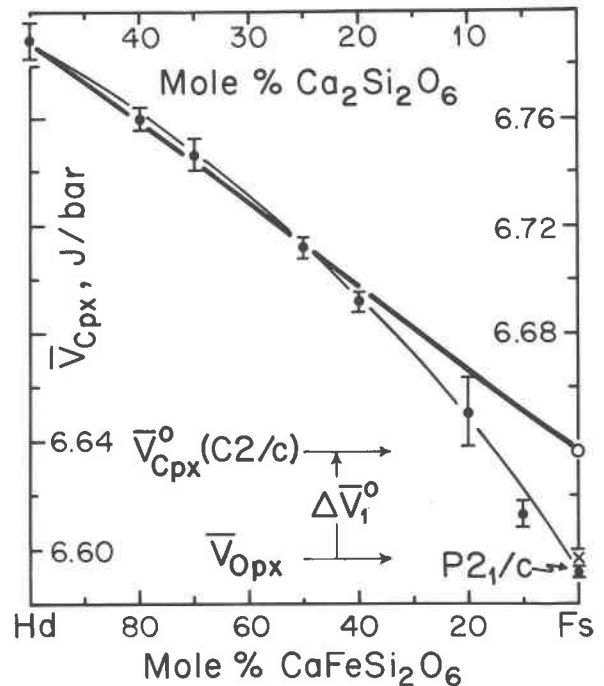


Fig. 4. Comparison of Hd-CFs unit-cell volumes measured at room temperature and pressure (symbols and light line, Lindsley *et al.*, 1969) and those calculated from the solution model for  $C2/c$  pyroxenes at elevated temperatures and pressures (heavy line). The calculated volumes agree well with measured volumes for Ca-rich compositions that are  $C2/c$  at room temperature, but deviate for Ca-poor phases that are  $P2_1/c$  at room temperature. The inset shows the derivation of the volume for pure  $C2/c$  CFs (circle) from that of OFs(X):  $\bar{V}_{\text{Cpx}}^{\circ}(C2/c) = \bar{V}_{\text{Opx}} + \Delta\bar{V}_1^{\circ}$ .

(*e.g.*, Mukhopadhyay and Lindsley, 1981), we should also be able to calculate Hd<sub>ss</sub>-Fa-Qtz equilibria using the present model, in conjunction with the OFs-Fa-Qtz data of Bohlen *et al.* (1980) and an olivine solution model. The experimental data obtained at high pressures for the Hd-Fs join would then become more directly applicable to crustal rocks—such as the Skaergaard Intrusion and a number of lunar basalts—that have undergone extreme iron enrichment.

#### Acknowledgments

This study took place over a number of years, and many people contributed to it. I especially thank Selena Dixon, Adrienne Labotka, and Clara Podpora for assistance in preparing starting minerals and microprobe sections; Paula Davidson, John Grover, and Allan Turnock for helpful discussions on the phase equilibria and thermodynamic properties of pyroxenes; Robert Muller for machining the high-pressure assemblies; Lois Koh for drafting the figures; and Shirley King for typing the manuscript and making it possible for my laboratory to function. Paula

Davidson, Alexandra Navrotsky, and Robert Newton improved the manuscript by their constructive criticisms. Work supported by National Science Foundation, Earth Sciences Section, NSF Grants EAR-7622129 and EAR-8026250.

### References

- Bohlen, S. R., Essene, E. J., and Boettcher, A. L. (1980) Reinvestigation and application of olivine-quartz-orthopyroxene barometry. *Earth and Planetary Science Letters*, 47, 1–10.
- Bowen, N. L., Schairer, J. F. Posnjak, E. (1933) The system, CaO–FeO–SiO<sub>2</sub>. *American Journal of Science*, 26, 193–284.
- Boyd, F. R., and England, J. L. (1963) Effect of pressure on the melting of diopside, CaMgSi<sub>2</sub>O<sub>6</sub>, and albite, NaAlSi<sub>3</sub>O<sub>8</sub>, in the range up to 50 kilobars. *Journal of Geophysical Research*, 68, 311–323.
- Davis, B. T. C., and Boyd, F. R. (1966) The join Mg<sub>2</sub>Si<sub>2</sub>O<sub>6</sub>–CaMgSi<sub>2</sub>O<sub>6</sub> at 30 kilobars pressure and its application to pyroxenes from kimberlites. *Journal of Geophysical Research*, 71, 3567–3576.
- Helgeson, H. C., Delaney, J. M., Nesbitt, H. W., and Bird, D. K. (1978) Summary and critique of the thermodynamic properties of the rock-forming minerals. *American Journal of Science*, 278A, 229p.
- Holland, T. J. B., Navrotsky, A., and Newton, R. C. (1979) Thermodynamic parameters of CaMgSi<sub>2</sub>O<sub>6</sub>–Mg<sub>2</sub>Si<sub>2</sub>O<sub>6</sub> pyroxenes based on regular solution and cooperative disordering models. *Contributions to Mineralogy and Petrology*, 69, 337–344.
- Lindsley, D. H. (1967) The join hedenbergite–ferrosilite at high pressures and temperatures. *Carnegie Institution of Washington, Year Book*, 65, 230–234.
- Lindsley, D. H. (1980) Phase equilibria of Ca–Mg–Fe pyroxenes at pressures greater than 1 atm. In C. T. Prewitt, Ed., *MSA Reviews in Mineralogy*, V. 7: Pyroxenes.
- Lindsley, D. H., and Burnham, C. W. (1970) Pyroxferroite: Stability and x-ray crystallography of synthetic Ca<sub>0.15</sub>Fe<sub>0.85</sub>SiO<sub>3</sub> pyroxenoid. *Science*, 168, 364–367.
- Lindsley, D. H. and Dixon, S. A. (1976) Diopside-enstatite equilibria at 850°–1400°C, 5–35 kbar. *American Journal of Science*, 276, 1285–1301.
- Lindsley, D. H., Grover, J. E., and Davidson, P. M. (1981) The thermodynamics of the Mg<sub>4</sub>Si<sub>2</sub>O<sub>6</sub>–CaMgSi<sub>2</sub>O<sub>6</sub> join: A review and an improved model. In S. K. Saxena, Ed., *Advances in Physical Geochemistry*, p. 146–172. Springer-Verlag, New York.
- Lindsley, D. H., MacGregor, I. D., and Davis, B. T. C. (1964) Synthesis and stability of ferrosilite. *Carnegie Institution of Washington Year Book*, 63, p. 174–176.
- Lindsley, D. H., and Munoz, J. L. (1969) Subsolidus relations along the join hedenbergite-ferrosilite. *American Journal of Science*, 267A (Schairer Volume), 295–324.
- Lindsley, D. H., Munoz, J. L., and Finger, L. W. (1969) Unit-cell parameters of clinopyroxenes along the join hedenbergite-ferrosilite. *Carnegie Institution of Washington Year Book*, 67, 91–92.
- Mukhopadhyay, D., and Lindsley, D. H. (1981) Miscibility gap in CaFeSiO<sub>4</sub>–Fe<sub>2</sub>SiO<sub>4</sub> system. *EOS*, 62, 412.
- Ohashi, Y., Burnham, C. W., and Finger, L. W. (1975) The effect of Ca–Fe substitution on the clinopyroxene crystal structure. *American Mineralogist*, 60, 423–34.
- Saxena, S. K., and Nehru, C. E. (1975) Enstatite-diopside solvus and geothermometry. *Contributions to Mineralogy and Petrology*, 49, 259–267.
- Thompson, J. B., Jr. (1967) Thermodynamic properties of simple solutions. In P. H. Abelson, Ed., *Researches in Geochemistry*, V. 2, p. 340–361.
- Turnock, A. E. (1962) Preliminary results on melting relations of synthetic pyroxenes on the diopside–hedenbergite join. *Carnegie Institution of Washington Year Book*, 61, 81–82.
- Turnock, A. C., Lindsley, D. H., and Grover, J. E. (1973) Synthesis and unit-cell parameters of Ca–Mg–Fe pyroxenes. *American Mineralogist*, 58, 50–59.

*Manuscript received, April 23, 1981.  
accepted for publication, July 15, 1981.*